AIP | Physics of Fluids

Free boundary fieldreversed configuration (FRC) equilibria in a conducting cylinder

Ross L. Spencer and Dennis W. Hewett

Citation: Physics of Fluids (1958-1988) **25**, 1365 (1982); doi: 10.1063/1.863901
View online: http://dx.doi.org/10.1063/1.863901
View Table of Contents: http://scitation.aip.org/content/aip/journal/pof1/25/8?ver=pdfcov
Published by the AIP Publishing

Articles you may be interested in
Hybrid equilibria of field-reversed configurations
Phys. Plasmas **18**, 112509 (2011); 10.1063/1.3660674

Profile consistency in equilibria of fieldreversed configurations
Phys. Fluids B **4**, 645 (1992); 10.1063/1.860262

Stabilization of the fieldreversed configuration (FRC) tilt instability with energetic ion beams
Phys. Fluids B **3**, 2609 (1991); 10.1063/1.859973

Experimental and computational equilibria of fieldreversed configurations
Phys. Fluids **28**, 1810 (1985); 10.1063/1.864924

Twodimensional equilibria of fieldreversed configurations in a perfectly conducting cylindrical shell
Phys. Fluids **26**, 1299 (1983); 10.1063/1.864291

This article is copyrighted as indicated in the article. Reuse of AIP content is subject to the terms at: http://scitationnew.aip.org/termsconditions. Downloaded to IP: 128.187.97.22 On: Tue, 15 Apr 2014 20:42:50

Free boundary field-reversed configuration (FRC) equilibria in a conducting cylinder

Ross L. Spencer and Dennis W. Hewett
University of California,, Los Alamos National Laboratory, Los Alamos, New Mexico 87545

(Received 9 February 1982; accepted 13 May 1982)

Highly elongated field-reversed configuration (FRC) equilibria are computed in a straight conducting cylinder for the pressure profile $p'(\psi) = cH(\psi)$, where $H(x)$ is the Heaviside function. The equilibria are found by inverting the Grad–Shafranov equation by means of a Green's function and by solving the resulting nonlinear integral equation. Long equilibria are obtained only for values of the constant c very near a critical value: the equilibria change from 2:1 elongated to infinitely long as c varies by only 0.3%. This criticial value of c is predicted by the average beta condition.

I. INTRODUCTION

Field-reversed theta-pinch experiments routinely produce very prolate plasma equilibria; magnetohydrodynamic equilibrium calculations do not. Since the experimental plasmas seem to be stable to the tilting instability that is predicted for moderately elongated equilibria, it has been suggested that the observed stability is due to exaggerated elongation. It has not been easy to test this hypothesis because very long equilibria have been difficult to compute. Previous calculations have indicated that such equilibria might exist, but none of these computed equilibria has been completely satisfactory. The equilibria of Berk, Hammer, and Weitzner[1] are the simplest to use in practical work, but these equilibria do not satisfy realistic boundary conditions outside the separatrix. In their model the region outside the separatrix is filled either with field lines containing high pressure plasma or with vacuum field lines that are distorted by the presence of external coils.[2] Byrne and Grossman proposed equilibria with an elliptical o point replaced by a slit on which the magnetic field vanishes.[3] It seems unlikely that slit equilibria exist because of the pathological conditions implied by having the stream function and both of its derivatives vanish along a line segment.[4] Christian has been able to produce elongated equilibria for a limited number of pressure profiles, but has difficulty computing the transition from short equilibria to long ones.[5] His work on very long equilibria for the pressure profile we consider here was very helpful to us, however.

The accurate solution of this difficult mathematical problem is the subject of this paper. We present a new approach to the computation of FRC equilibria that avoids the previously encountered difficulties. This method is most useful for the pressure profile used by Berk *et al.*[1]; in fact, we have determined what Berk–Hammer–Weitzner equilibria would look like if the vacuum field lines outside the separatrix were required to be parallel to a conducting cylinder.

We solve the Grad–Shafranov equation,

$$r\frac{\partial}{\partial r}\left(\frac{1}{r}\frac{\partial \psi}{\partial r}\right) + \frac{\partial^2\psi}{\partial z^2} = \Delta^*\psi = -r^2p'(\psi), \tag{1}$$

where ψ is the poloidal flux function, $p'(\psi) = d\,p(\psi)/d\psi$, and where $p(\psi)$ is the pressure on the magnetic surface labeled by ψ. We solve Eq. (1) in an infinitely long, flux-conserving cylinder of radius a; the boundary conditions are $\psi(a,z) = -\psi_w$ and $\partial\psi/\partial z = 0$ as $|z|$ approaches infinity. The pressure profile is

$$p'(\psi) = cH(\psi), \tag{2}$$

where c is a constant and where $H(x)$ is the Heaviside function. Note that $cH(\psi) = -j_\theta/r$, where j_θ is the toroidal current density. We have found four solutions to this problem: a vacuum solution, two z-independent plasma solutions, and an r-z-dependent plasma solution. These last three solutions are obtained only if the constant c is greater than a certain minimum value, c_1; for c smaller than c_1 the three plasma solutions cease to exist. At c_1 the two z-independent plasma solutions coalesce; at a slightly higher critical value of c, c_2, the two-dimensional solution and one of the z-independent plasma solutions coalesce. Two-dimensional equilibria are obtained for c above c_2. For large values of c these equilibria consist of small spheres of fluid; as c approaches c_2 from above, the equilibria rapidly become very long and racetrack-like in shape. At c_2 they become infinitely long. This sharply singular transition from two-dimensional equilibria to one-dimensional equilibria and the notorious difficulty of computing near a bifurcation point probably explain why elongated solutions have been so difficult to find.

II. ONE-DIMENSIONAL SOLUTIONS

Except for the trivial vacuum solution, $\psi = -\psi_w r^2/a^2$, the z-independent plasma solutions are the simplest to find. An elementary calculation yields

$$\psi = \begin{cases} \frac{1}{2}r^2(b - \frac{1}{2}cr^2), & r \leqslant r_{\text{sep}}, \\ -\frac{1}{2}br^2 + d, & r_{\text{sep}} < r < a, \end{cases} \tag{3}$$

where

$$b = (a^2c/8)[1 \pm (1 - 32\psi_w/ca^4)^{1/2}], \tag{4}$$

and where $d = 2b^2/c$ and $\psi = 0$ at $r_{\text{sep}} = 2(b/c)^{1/2}$. Note that there are two possible solutions; these two solutions are realized only if b is real, i.e., only if $c \geqslant c_1 = 32\psi_w/a^4$. Figure 1 displays the $\psi = 0$ radius as a function of c. The upper solution in this figure is a high-trapped-flux solution that compresses the vacuum flux against the wall as c becomes large. The lower solution in this figure is a low-trapped-flux

 0031-9171/82/081365-05$01.90 © 1982 American Institute of Physics

This article is copyrighted as indicated in the article. Reuse of AIP content is subject to the terms at: http://scitationnew.aip.org/termsconditions. Downloaded to IP: 128.187.97.22 On: Tue, 15 Apr 2014 20:42:50

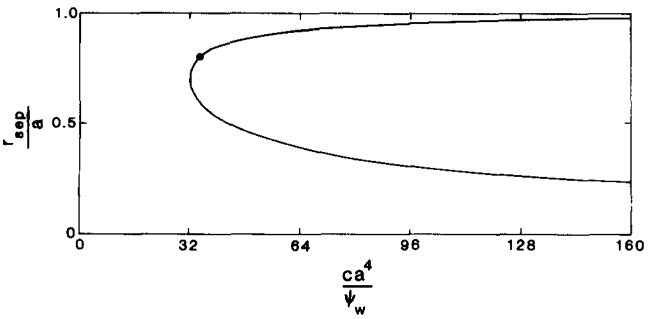

FIG. 1. The $\psi = 0$ radius is displayed as a function of c for the one-dimensional solution of the model problem. The dot on the upper branch at $c = c_2 = 36\psi_w/a^4$ locates the point where the two-dimensional solutions connect with the one-dimensional solutions.

solution that is squeezed to the axis by the vacuum flux as c becomes large.

The presence of a value of c below which no equilibria exist is explained by noting that the toroidal current density is given by $j_\theta = -crH(\psi)$. If c is too small, there is not enough current density to produce field reversal, and no solutions of the model problem are possible. This argument also applies to two-dimensional solutions, so we expect in any family of equilibria parameterized by c to encounter a lower limit below which equilibria no longer exist.

All of the one-dimensional solutions have the property that $\langle \beta \rangle = \frac{2}{3}$ where

$$\langle \beta \rangle = \frac{2}{r_{\rm sep}^2} \int_0^{r_{\rm sep}} \left(\frac{2p}{B_0^2} \right) r\, dr, \tag{5}$$

and where B_0 is the magnetic field at $r = a$. Hence, the only one-dimensional equilibrium that satisfies the average beta condition of Barnes,[6,7] $\langle \beta \rangle = 1 - \frac{1}{2}(r_{\rm sep}/a)^2$, is the one with $r_{\rm sep} = (2/3)^{1/2}a$. This equilibrium is on the high-trapped-flux branch at $c = c_2 = 36\psi_w/a^4$ as indicated in Fig. 1. Any long two-dimensional equilibrium must resemble this special one-dimensional equilibrium, i.e., must have about the same values of c, $r_{\rm sep}$, and trapped flux.

III. TWO-DIMENSIONAL SOLUTIONS

From our studies of Hill's vortex equilibria we know there is at least one two-dimensional family of solutions parameterized by c. With ψ given by the Hill's vortex formula inside the separatrix, a matching vacuum field outside the separatrix may be constructed by means of spheroidal coordinates. This calculation is discussed in more detail in the Appendix. For both prolate and oblate Hill's vortices, the matching vacuum field has mirror coils at infinity, but for the spherical Hill's vortex, the field lines at infinity are straight. This spherical solution is given by

$$\psi = \begin{cases} \frac{3}{4}B_0 r^2[1-(r^2+z^2)/\rho_0^2], & r^2+z^2<\rho_0^2, \\ -\frac{1}{2}B_0 r^2\{1-[\rho_0^2/(r^2+z^2)]^{3/2}\}, & r^2+z^2 \geqslant \rho_0^2, \end{cases} \tag{6}$$

where $\rho_0 = (15B_0/2c)^{1/2}$, and where B_0 is the uniform magnetic field at infinity. This solution will be obtained in our model problem when the plasma radius becomes very small so that the cylindrical wall is effectively very far away, i.e., when c is very large. This means there exists a two-dimensional family of solutions whose large c limit is given by Eq. (6) (B_0 is replaced by $2\psi_w/a^2$.) As c is decreased, the equilibria should become larger and finally approach a final state at $c = c_2$, as required by the average beta condition.

To accurately describe this transition from small spherical equilibria to elongated equilibria we solve the problem by using a Green's function technique. By means of the Green's theorem for Δ^*,

$$\int (f\Delta^* g - g\Delta^* f)\frac{dV}{r^2} = \int (f\nabla g - g\nabla f)\cdot\frac{d\mathbf{a}}{r^2}, \tag{7}$$

the Grad–Shafranov equation may be inverted to obtain the equation

$$\psi = -\int G(r,r',z,z')\,p'(\psi)r'\,dr'\,dz' + \frac{1}{2\pi}\int \psi \frac{\partial G}{\partial r'}\frac{da'}{r'^2}, \tag{8}$$

where G satisfies $\Delta^* G = r\delta(r-r')\delta(z-z')$ and $G = 0$ if r or $r' = a$. The Green's function is given by the expression

$$G(r,r',z,z') = \frac{rr'}{\pi}\int_0^\infty \cos[k(z-z')] \times I_1(kr)I_1(kr')[K_1(ka)/I_1(ka)]dk - \frac{(rr')^{1/2}}{2\pi} Q_{1/2}\left(\frac{r^2+r'^2+(z-z')^2}{2rr'}\right), \tag{9}$$

where $I_1(x)$ and $K_1(x)$ are modified Bessel functions and where $Q_{1/2}(x)$ is the Legendre function of the second kind with degree one-half.

Formulating the problem this way has the advantage that it is not necessary to compute finite differences across the separatrix where the current density may be discontinuous; the integration is taken only over the region where there is current. Doing the integrations accurately requires many integration points; if a general pressure profile were used, iteration would be necessary to find ψ inside the separatrix, and this method would be very expensive. But for our model problem, there is no ψ dependence on the right-hand side of Eq. (8) except for the shape of the separatrix. Since the separatrix is given by $\psi = 0$, Eq. (8) can be used to obtain the following nonlinear equation for the shape of the separatrix.

$$c\int_\Omega G r'\,dr'\,dz' + \psi_w \frac{r^2}{a^2} = 0, \tag{10}$$

where Ω is the region in the $r' - z'$ plane bounded by the separatrix.

We do the integrations in spherical coordinates and represent the separatrix as an expansion in even-order Legendre polynomials as follows:

$$\rho(x) = \sum_{n=1}^{N} a_n P_{2n}(x), \tag{11}$$

where $\rho(x)$ is the spherical radius of the separatrix at the polar angle $\theta = \cos^{-1}(x)$. The problem is solved when the a_n's are determined. To solve Eq. (10) we rearrange it so that the explicit r^2 is isolated, substitute $r = \rho\sin\theta$ using ρ from Eq. (11), and integrate over x with a Legendre polynomial to

This article is copyrighted as indicated in the article. Reuse of AIP content is subject to the terms at: http://scitationnew.aip.org/termsconditions. Downloaded to IP: 128.187.97.22 On: Tue, 15 Apr 2014 20:42:50

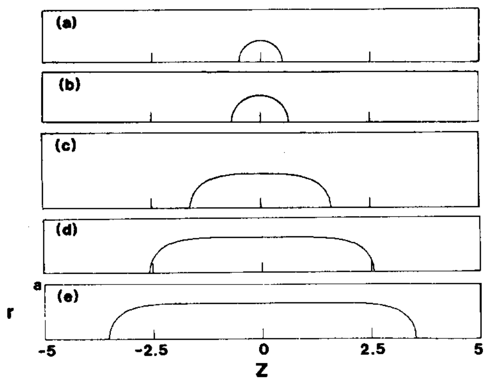

FIG. 2. The separatrix shapes for a sequence of values of V/a^3 are shown: (a) 0.5, (b) 1, (c) 5, (d) 9, (e) 13.

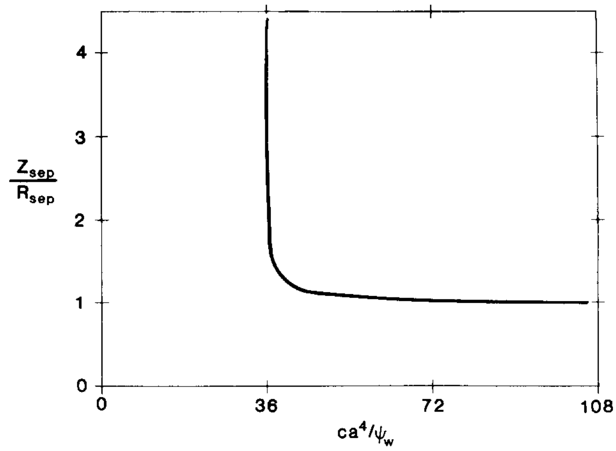

FIG. 3. The elongation, z_{sep}/r_{sep}, is displayed as a function of c.

obtain the following set of N nonlinear equations for the a_n's.

$$a_n = \left(2n + \frac{1}{2}\right) a \left(\frac{c}{\psi_w}\right)^{1/2} \int_{-1}^{1} \frac{P_{2n}(x)}{(1-x^2)^{1/2}} \times \left(\int_\Omega \mathrm{G}r'\,\mathrm{d}r'\,\mathrm{d}z'\right)^{1/2} dx, \quad n = 1,2,\ldots,N. \tag{12}$$

Note that the right-hand side of Eq. (12) depends on the a_n's both through the shape of the integration region,

$$\int_\Omega r'\,dr'\,dz' = \int_{-1}^{1} dx' \int_0^{\rho(x)} \rho'^2\,d\rho', \tag{13}$$

and through the dependence of G on $r = \rho \sin\theta$ and $z = \rho\cos\theta$. With c fixed, this is just a system of nonlinear equations to solve; the problem can be solved this way but, because of the singular behavior of the solution as c is varied, it is helpful to let c also be one of the variables to be determined and to add one more equation to the system. We do this by requiring that the separatrix enclose volume V. The extra equation is

$$\frac{2\pi}{3}\int_{-1}^{1} \rho^3(x)dx = V. \tag{14}$$

We use the multivariable nonlinear equation solver "C05NAF" in the NAG library[8] to solve for the a_n's and c given V and the boundary conditions.

When Eqs. (12) and (14) are solved for small values of V, the small radius spherical solution is recovered. As V is increased the solutions remain practically spherical until the radius of the solution at $z = 0$ becomes greater than about $0.6a$; as V is increased further, the solutions become prolate and racetrack-like in shape. As the volume becomes large enough that the elongation of the equilibria (defined as the ratio of the half-length to the maximum radius) is greater than about 2, c rapidly approaches c_2; the two-dimensional solution branch connects with the one-dimensional high-trapped-flux solution branch at the place where the average beta condition is satisfied. Figure 2 shows the separatrix shapes for an increasing sequence of values of V, Fig. 3 shows the elongation of the solutions as a function of c, and Fig. 4 shows the flux plot of a long equilibrium. Note that the elongation is sharply singular at the critical value of c; only in a narrow region in c are long equilibria obtained. Since these elongated equilibria lie near a bifurcation point, it is a very delicate matter to compute them by standard numerical methods.

IV. CONCLUSION

We have found FRC equilibria under the conditions that $dp/d\psi$ be a constant inside the separatrix and that there be a vacuum field outside the separatrix with field lines parallel to a cylindrical wall. Equilibria of any desired elongation may be found, but as the elongation becomes greater than about 2, these equilibria can roughly be described as having a long one-dimensional section in the middle and a transition region from one-dimensional plasma to one-dimensional vacuum at each end. The shape of the field lines in the transition region is the same for all equilibria with elongations above 2. Thus, the freedom in the Berk–Hammer–Weitzner equilibrium model[1] to choose both the elongation and the shape of the separatrix near the field nulls is restricted by the requirement that the field lines outside the separatrix satisfy conducting wall boundary conditions. To change the shape of the transition region it would be necessary either to change the boundary conditions or to change the pressure profile.

Finally, we propose the following prescription for find-

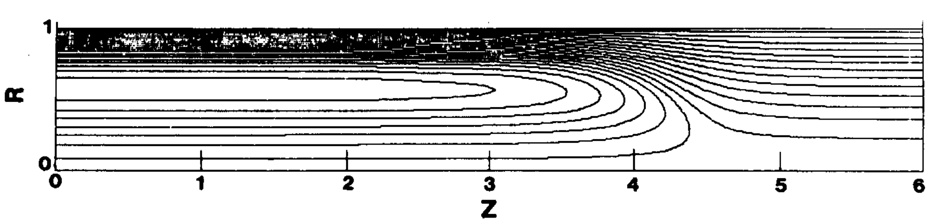

FIG. 4. A flux plot for the case $V = 13a^3$ is shown.

This article is copyrighted as indicated in the article. Reuse of AIP content is subject to the terms at: http://scitationnew.aip.org/termsconditions. Downloaded to IP: 128.187.97.22 On: Tue, 15 Apr 2014 20:42:50

ing highly elongated FRC equilibria. Choose a pressure profile and choose boundary conditions outside the separatrix. Let one of the parameters in the chosen pressure profile be a variable and impose a global constraint such as specifying the volume or the total toroidal current enclosed by the separatrix. Solve for the flux surfaces and the free parameter in the pressure profile. In a future publication we shall present examples of this procedure. We propose this recipe because we believe that the sharp singularity in the elongation as a function of the parameter c in our pressure profile will occur with parameters in other pressure profiles. Such a sharp singularity makes looking for long equilibria by varying parameters in pressure profiles a very delicate matter.

ACKNOWLEDGMENTS

We thank R. Christian for stimulating and useful discussions, and we thank T. Hewitt for numerical work on the appendix.

This work was performed under the auspices of the U.S.D.O.E.

APPENDIX

The simplest two-dimensional model for an FRC is the Hill's vortex,

$$\psi = \frac{\psi_0}{ab} r^2\left(1 - \frac{r^2}{a^2} - \frac{z^2}{b^2}\right). \tag{A1}$$

Unfortunately, in this model all space is filled with conducting fluid. A more realistic model may be obtained from the Hill's vortex by letting the field inside the separatrix be given by Eq. (A1) and by computing a matching vacuum field outside the separatrix. (The calculation of this vacuum field has also been done independently by Kaneko *et al.*[9] and by John Boyd.[10]) The calculation of the vacuum field is made relatively simple by the ellipsoidal shape of the separatrix, which makes it natural to compute the field by means of spheroidal coordinates.[11] There are three cases to consider: (1) a prolate separatrix, $b > a$, (2) an oblate separatrix, $b < a$, and (3) a spherical separatrix, $b = a$.

1. Prolate separatrix

The prolate spheroidal coordinates (μ,θ) are connected to the cylindrical coordinates (r,z) by the following relations:

$$r = d \sinh\mu \sin\theta, \qquad z = d\cosh\mu\cos\theta, \tag{A2}$$

where $d = (b^2 - a^2)^{1/2}$. In these coordinates the separatrix is described by

$$\mu = \mu_0 = \tanh^{-1}(a/b). \tag{A3}$$

In the vacuum, ψ satisfies the equation $\Delta^*\psi = 0$, which reduces to the equation

$$\sinh\mu \frac{\partial}{\partial\mu}\left(\frac{1}{\sinh\mu}\frac{\partial\psi}{\partial\mu}\right) + \sin\theta\frac{\partial}{\partial\theta}\left(\frac{1}{\sin\theta}\frac{\partial\psi}{\partial\theta}\right) = 0. \tag{A4}$$

This equation is separable and solutions can be constructed by superposition as usual. Requiring that ψ and its normal

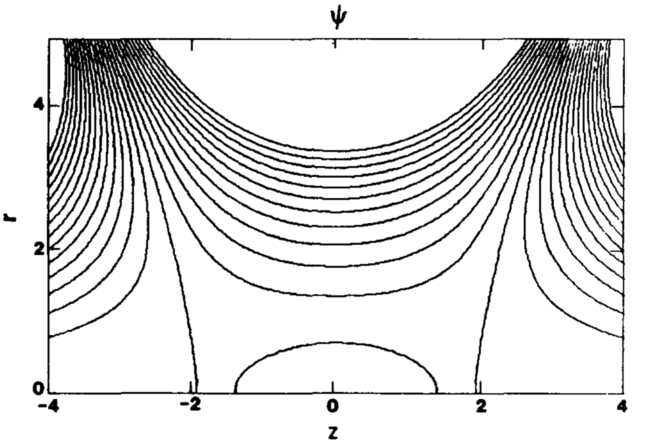

FIG. 5. The vacuum field lines are displayed for a prolate Hill's vortex with $z_{sep}/r_{sep} = 2$.

derivative be continuous at the separatrix yields the following formula for ψ in the vacuum.

$$\psi = q_1 S_1^1(\mu,\theta) + q_3 S_3^1(\mu,\theta), \tag{A5}$$

where

$$S_n^1(\mu,\theta) = \sinh\mu \sin\theta P_n^1(\cos\theta) \times\left(\frac{P_n^1(x)}{P_n^1(x_0)} - \frac{Q_n^1(x)}{Q_n^1(x_0)}\right), \tag{A6}$$

and where $x = \cosh\mu$ and $x_0 = \cosh\mu_0$. The coefficients q_1 and q_3 are given by

$$q_1 = -\psi_0(\tfrac{4}{5} + a^2/5b^2) P_1^1(x_0)Q_1^1(x_0), \tag{A7}$$

$$q_3 = (\psi_0/45)(1 - a^2/b^2) P_3^1(x_0)Q_3^1(x_0). \tag{A8}$$

The functions $P_n^1(x)$ and $Q_n^1(x)$ are associated Legendre functions.[12] Figure 5 displays contours of constant ψ outside the separatrix for a prolate Hill's vortex with $b/a = 2$.

2. Oblate separatrix

The prolate spheroidal coordinates (ν,ϕ) are connected to the cylindrical coordinates (r,z) by the following relations:

$$r = g\cosh\nu\sin\phi, \qquad z = g\sinh\nu\cos\phi, \tag{A9}$$

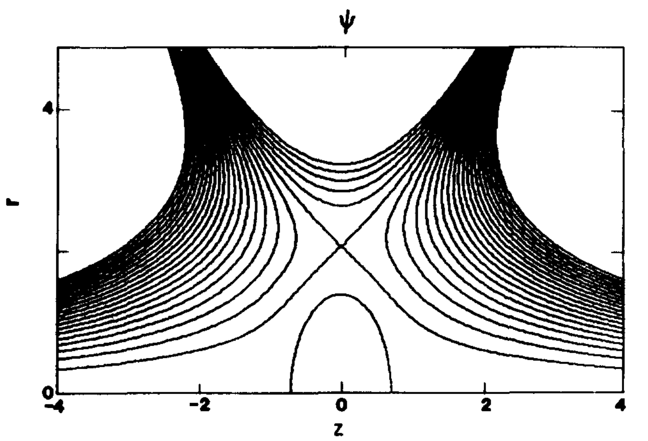

FIG. 6. The vacuum field lines are displayed for an oblate Hill's vortex with $z_{sep}/r_{sep} = 0.5$.

This article is copyrighted as indicated in the article. Reuse of AIP content is subject to the terms at: http://scitationnew.aip.org/termsconditions. Downloaded to IP: 128.187.97.22 On: Tue, 15 Apr 2014 20:42:50

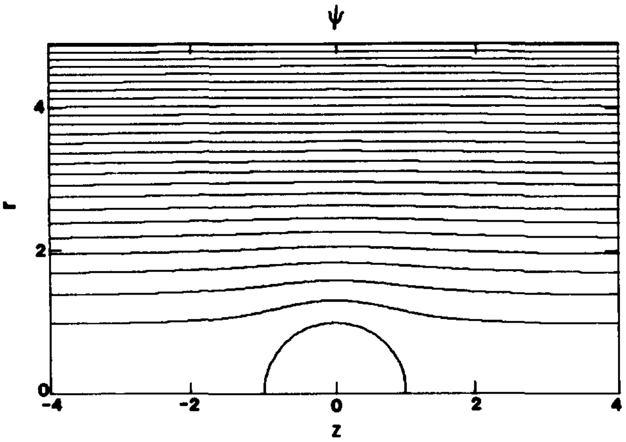

FIG. 7. The vacuum field lines are displayed for a spherical Hill's vortex.

where $g = (a^2 - b^2)^{1/2}$. The separatrix is described by

$$\nu = \nu_0 = \tanh^{-1}(b/a). \tag{A10}$$

The flux function satisfies the equation

$$\cosh\nu \frac{\partial}{\partial\nu}\left(\frac{1}{\cosh\nu}\frac{\partial\psi}{\partial\nu}\right) + \sin\phi\frac{\partial}{\partial\phi}\left(\frac{1}{\sin\phi}\frac{\partial\psi}{\partial\phi}\right) = 0, \tag{A11}$$

and the vacuum solution is

$$\psi = r_1 T_1^1(\nu,\phi) + r_3 T_3^1(\nu,\phi), \tag{A12}$$

where

$$T_n^1(\nu,\phi) = \cosh\nu\sin\phi\, P_n^1(\cos\phi) \times\left(\frac{P_n^1(iy)}{P_n^1(iy_0)} - \frac{Q_n^1(iy)}{Q_n^1(iy_0)}\right), \tag{A13}$$

and where $y = \sinh\nu$, $y_0 = \sinh\nu_0$, and $i = (-1)^{1/2}$. The coefficients r_1 and r_3 are given by

$$r_1 = \psi_0(\tfrac{4}{5} + a^2/5b^2)\, P_1^1(iy_0)Q_1^1(iy_0), \tag{A14}$$

$$r_3 = (\psi_0/45)(a^2/b^2 - 1)\, P_3^1(iy_0)Q_3^1(iy_0). \tag{A15}$$

Figure 6 displays contours of constant ψ outside the separatrix for a prolate Hill's vortex with $b/a = 0.5$.

3. Spherical separatrix

The vacuum field in this case may be gotten either by using spherical coordinates or by allowing a and b to approach each other in the formulas of Secs. 1 or 2. In any case the result is that in the vacuum

$$\psi = -\frac{2}{3}\psi_0\frac{r^2}{a^2}\left[1 - \left(\frac{a^2}{r^2+z^2}\right)^{3/2}\right]. \tag{A16}$$

Figure 7 shows the vacuum field lines for this case. Note that only for this spherical case are straight field lines obtained infinitely far from the separatrix.

[1] H. L. Berk, J. H. Hammer, and H. Weitzner, Phys. Fluids **24**, 1758 (1981).
[2] D. V. Anderson, J. H. Hammer, and D. C. Barnes, in *Proceedings of the Fourth Symposium on the Physics and Technology of Compact Toroids* (Lawrence Livermore National Laboratory, Livermore, California, 1981).
[3] R. N. Byrne and W. Grossman, in *Proceedings of the Third Symposium on Physics and Technology of Compact Toroids in the Magnetic Fusion Energy Program* (Los Alamos Scientific Laboratory, Los Alamos, NM, 1980), p. 138.
[4] D. V. Anderson and J. H. Hammer, in *Proceedings of the 1981 Sherwood Meeting* (Institute for Fusion Studies, University of Texas at Austin, Austin, TX 1981), 2C11.
[5] R. Christian (private communication).
[6] D. C. Barnes, C. E. Seyler, and D. V. Anderson, in *Proceedings of the US-Japan Joint Symposium on Compact Toruses and Energetic Particle Injection* (Plasma Physics Laboratory, Princeton, NJ, 1979), p. 110.
[7] W. T. Armstrong, R. K. Linford, J. Lipson, D. A. Platts, and E. G. Sherwood, Phys. Fluids **24**, 2068 (1981).
[8] *NAG Fortran Library Manual* [NAG (USA) Inc., Downers Grove, IL, 1976], subroutine CO5NAF.
[9] S. Kaneko, K. Chiyoda, and I. Hirota, J. Phys. Soc. Japan **50**, 359 (1981).
[10] J. Boyd (private communication).
[11] P. M. Morse and H. Feshbach, *Methods of Theoretical Physics* (McGraw-Hill, New York, 1953), Part 1, p. 661.
[12] M. Abramowitz and I. A. Stegun, *Handbook of Mathematical Functions* (Dover, New York, 1972), Chap. 8.

This article is copyrighted as indicated in the article. Reuse of AIP content is subject to the terms at: http://scitationnew.aip.org/termsconditions. Downloaded to IP: 128.187.97.22 On: Tue, 15 Apr 2014 20:42:50